

Supporting Information for:

Influence of alcoholic solvent and acetate anion coordination mode variations on structures and magnetic properties of heterometallic Zn₂Dy₂ tetrานuclear clusters

Hongshan Ke,^{*†} Wen Wei,[†] Yi-Quan Zhang,^{*‡} Jun Zhang,[#] Gang Xie[†] and Sanping Chen[†]

[†]Key Laboratory of Synthetic and Natural Functional Molecule Chemistry of Ministry of Education, College of Chemistry and Materials Science, Northwest University, Xi'an 710069, P. R. China. E-mail: hske@nwu.edu.cn; sanpingchen@126.com

[‡]Jiangsu Key Laboratory for NSLSCS, School of Physical Science and Technology, Nanjing Normal University, Nanjing 210023, P. R. China. E-mail: zhangyiquan@njnu.edu.cn

[#]School of Materials and Chemical Engineering, Anhui Jianzhu University, Hefei, 230601, P. R. China.

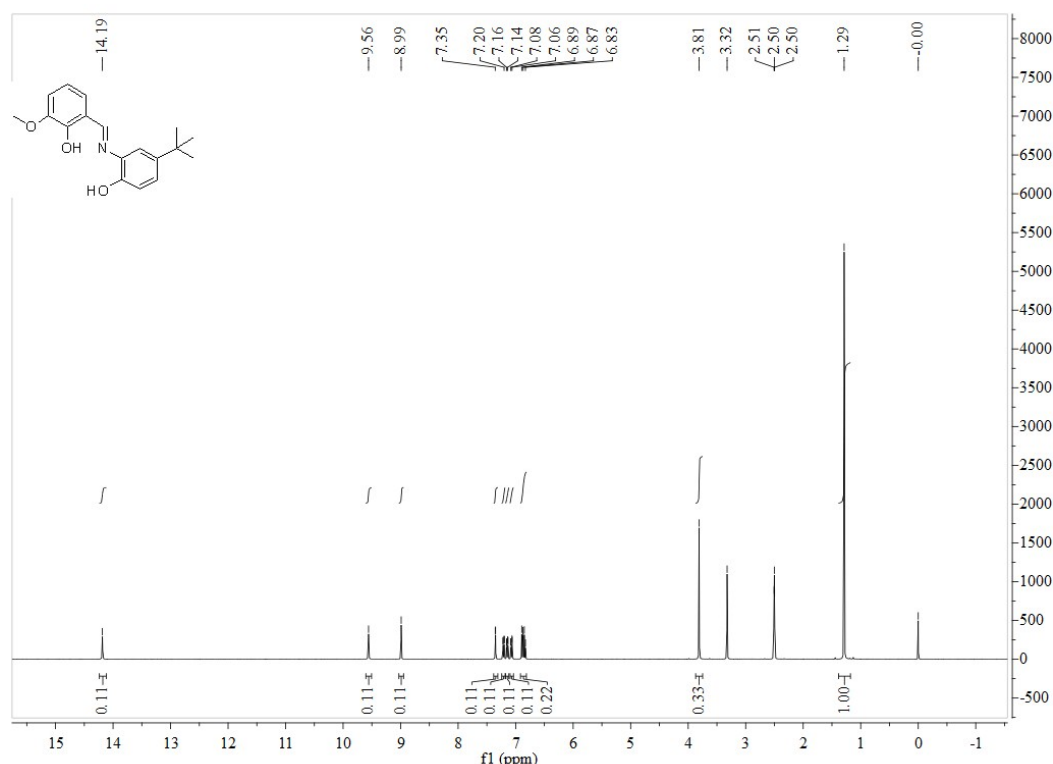
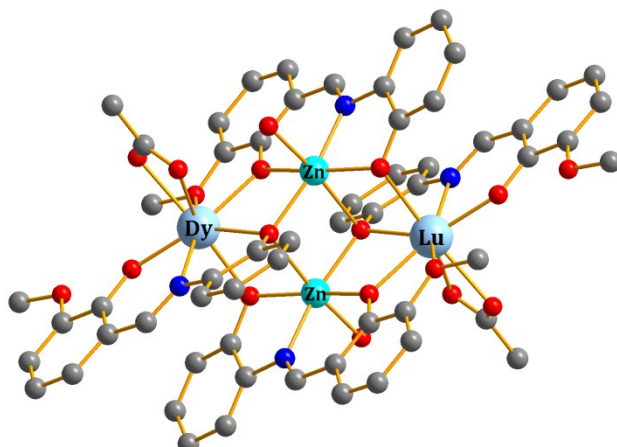


Figure S1. ¹H NMR spectrum of the ligand H₂L (400 MHz, d₆-DMSO, 298 K).

Table S1. Selected bond lengths (\AA) and angles ($^\circ$) for compounds **1** and **2**.

1	Bond lengths (\AA)		2
Zn(1)-N(2)	2.066(4)	Zn(1)-N(2)	2.073(4)
Zn(1)-O(3)#1	2.091(3)	Zn(1)-O(3)#2	2.076(3)
Zn(1)-O(3)	2.262(4)	Zn(1)-O(3)	2.258(3)
Zn(1)-O(5)	2.060(3)	Zn(1)-O(5)	2.081(3)
Zn(1)-O(6)	2.068(3)	Zn(1)-O(6)	2.107(3)
Zn(1)-O(9)	2.131(4)	Zn(1)-O(7)#2	2.080(3)
Dy(1)-N(1)	2.465(4)	Dy(1)-N(1)	2.454(4)
Dy(1)-O(2)	2.155(4)	Dy(1)-O(2)	2.229(3)
Dy(1)-O(3)	2.385 (3)	Dy(1)-O(3)	2.437(3)
Dy(1)-O(4)#1	2.505(4)	Dy(1)-O(4)#2	2.559(3)
Dy(1)-O(5) #1	2.297(3)	Dy(1)-O(5)	2.293(3)
Dy(1)-O(6)	2.344(4)	Dy(1)-O(6)	2.348(3)
Dy(1)-O(7)	2.430(4)	Dy(1)-O(8)	2.342(3)
Dy(1)-O(8)	2.443(4)	Dy(1)-O(9)	2.412(3)
Zn(1)…Zn(1)#1	3.2730(11)	Zn(1)…Zn(1)#1	3.3122(7)
Dy(1)…Zn(1)	3.5193(8)	Dy(1)…Zn(1)	3.5983(9)
Dy(1)…Zn(1)#1	3.4965(6)	Dy(1)…Zn(1)#2	3.4223(6)
Dy(1)…Dy(1)#1	6.2057(8)	Dy(1)…Dy(1)#2	6.1927(7)
Bond angles ($^\circ$)			
Zn(1)-O(3)-Zn(1)#1	97.41(13)	Zn(1)-O(3)-Zn(1)#2	99.61(12)
Zn(1)-O(3)-Dy(1)	98.43(12)	Zn(1)-O(3)-Dy(1)	99.98(11)
Zn(1)#1-O(3)-Dy(1)	102.55(14)	Zn(1)#2-O(3)-Dy(1)	98.31(11)
Zn(1)#1-O(5)#1-Dy(1)	106.61(14)	Zn(1)#2-O(5)#2-Dy(1)	102.86(12)
Zn(1)-O(6)-Dy(1)	105.63(14)	Zn(1)-O(6)-Dy(1)	107.62(12)

Symmetry transformations used to generate equivalent atoms: **1** and **2** #1 1-x, 1-y, -z,
#2 2-x, 2-y, 1-z.

**Figure S2.** Calculated model structure of individual Dy^{III} fragment of **1**; H atoms are omitted.

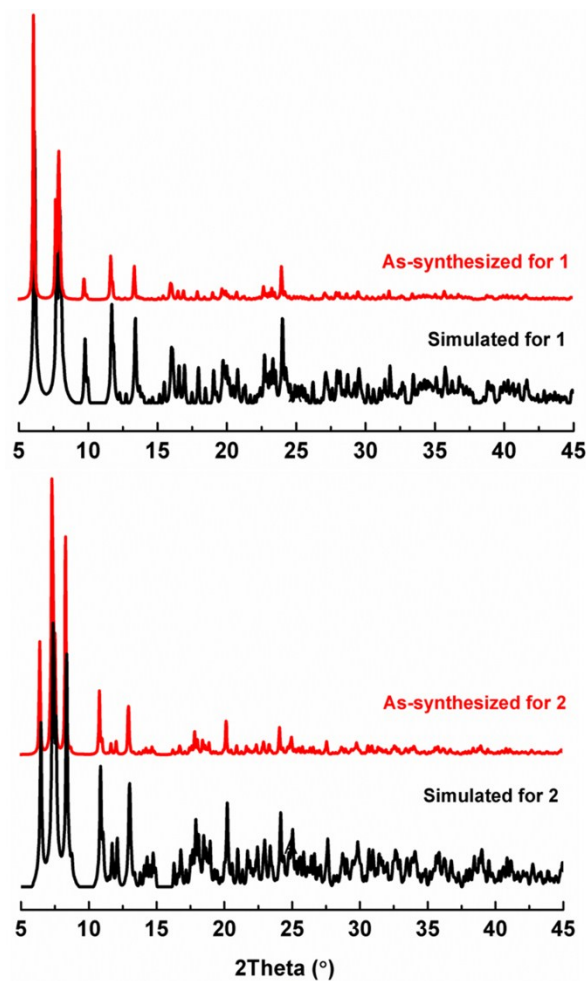


Figure S3. Comparing the simulated PXRD (black) and experimental patterns of compounds **1** and **2**.

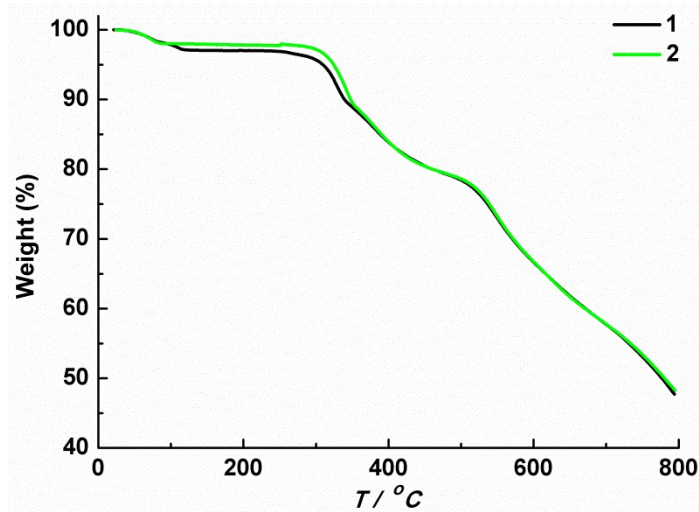
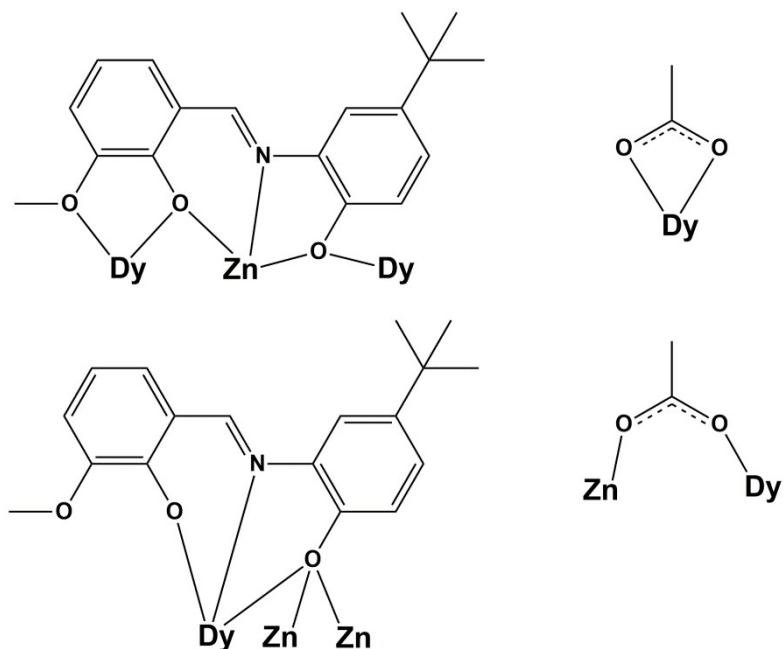


Figure S4. The TGA curve for **1** and **2**.

Table S2. SHAPE¹ analysis of compounds **1** and **2**.

Complex	Metal	HPBY (D _{6h})	CU (O _h)	SAPR (D _{4d})	TDD (D _{2d})	JGBF (D _{2d})	JETBPY (D _{3h})	JBTPR (C _{2v})	BTPR (C _{2v})	JSD (D _{2d})
1	Dy1	15.048	10.425	3.041	2.596	13.154	26.675	2.764	2.331	4.251
2	Dy1	12.993	9.172	2.299	1.551	11.983	27.709	2.040	1.766	4.400

Abbreviations: HPBY-Hexagonal bipyramidal, CU-Cube, SAPR-Square antiprism, TDD-Triangular dodecahedron, JGBF-Johnson-Gyrobifastigium J26, JETBPY-Johnson elongated triangular bipyramid J14, JBTPR-Johnson biaugmented trigonal prism J50, BTPR-Biaugmented trigonal prism, JSD-Snub diphenoid



Scheme S1. Different coordination modes of the ligand and acetate anion observed in compounds **1** and **2**.

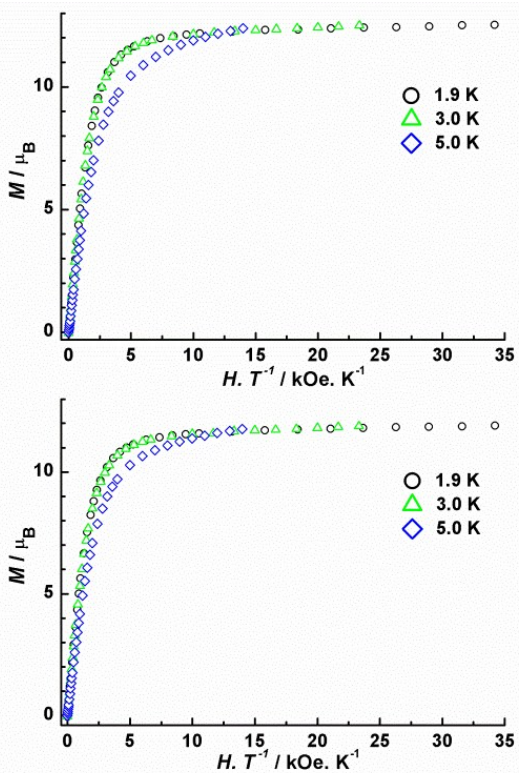


Figure S5. Field dependence of the reduced magnetization for **1** (top) and **2** (bottom) at 1.9, 3 and 5 K.

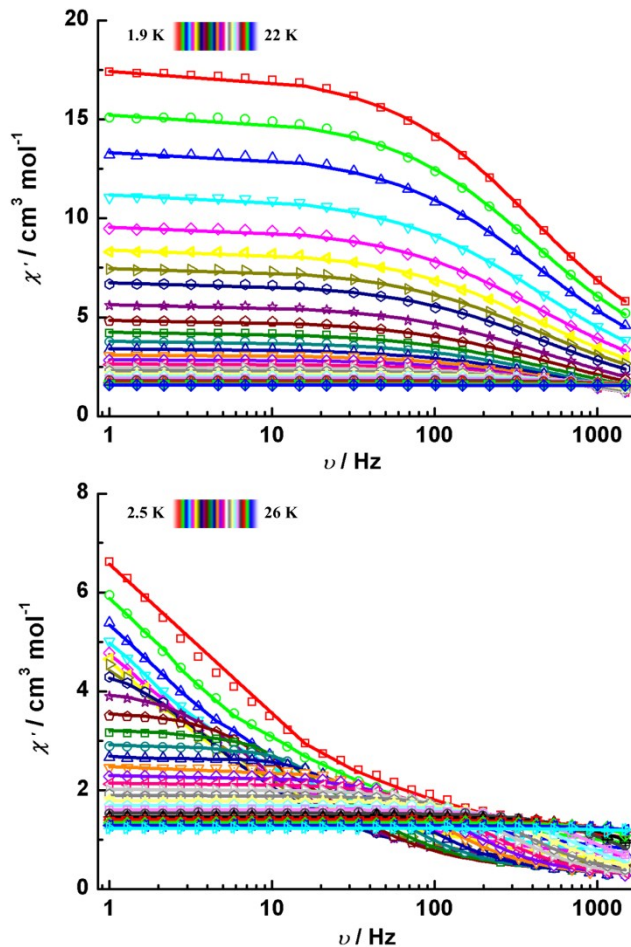


Figure S6. Frequency dependence of in-phase (χ'_M) components of the ac magnetic susceptibility signals for **1**(top) and **2** (bottom) under zero applied dc field and an oscillating field of 3.5 Oe. The colored solid lines are fits to a single Debye model.²

Table S3. χ_T , χ_S , τ and α values of **1** and **2** estimated by theoretical calculations on the basis of the generalized Debye model.²

1								
T/K	1.9	2.2	2.5	3	3.5	4	4.5	5
$\chi_T/\text{cm}^3 \text{mol}^{-1}$	17.54	15.32	13.42	11.28	9.63	8.45	7.53	6.80
$\chi_S/\text{cm}^3 \text{mol}^{-1}$	2.18	1.96	1.59	1.14	1.15	1.00	0.91	0.76
$\tau/\mu\text{sec}$	386.6	382.4	367.4	352.1	358.7	351.3	350.6	335.3
α	0.31	0.31	0.32	0.34	0.33	0.33	0.33	0.33
T/K	6	7	8	9	10	11	12	13
$\chi_T/\text{cm}^3 \text{mol}^{-1}$	5.68	4.89	4.28	3.80	3.44	3.12	2.87	2.65
$\chi_S/\text{cm}^3 \text{mol}^{-1}$	0.58	0.45	0.47	0.33	0.26	0.35	0.39	0.40
$\tau/\mu\text{sec}$	319.6	291.8	293.6	259.1	229.9	226.9	216.7	184.1
α	0.34	0.35	0.33	0.33	0.33	0.31	0.29	0.27
T/K	14	15	16	17	18	19	20	21
$\chi_T/\text{cm}^3 \text{mol}^{-1}$	2.46	2.30	2.14	2.02	1.91	1.80	1.72	1.63
$\chi_S/\text{cm}^3 \text{mol}^{-1}$	0.30	0.28	0.54	0.58	0.61	0.45	0.28	0.05

$\tau/\mu\text{sec}$	140.1	103.6	98.2	71.6	45.9	35.4	14.5	10.9
α	0.25	0.23	0.15	0.12	0.12	0.12	0.11	0.07
T/K	22							
$\chi_T/\text{cm}^3 \text{ mol}^{-1}$	1.57							
$\chi_S/\text{cm}^3 \text{ mol}^{-1}$	0.04							
$\tau/\mu\text{sec}$	6.53							
α	0.04							
				2				
T/K	2.5	3.0	3.5	4	4.5	5	6	7
$\chi_T/\text{cm}^3 \text{ mol}^{-1}$	20.94	19.7	16.81	13.99	10.97	9.0	6.86	4.78
$\chi_S/\text{cm}^3 \text{ mol}^{-1}$	0.59	0.52	0.47	0.43	0.41	0.40	0.37	0.36
τ/sec	1.8	1.75	1.24	0.77	0.39	0.19	0.074	0.0274
α	0.63	0.62	0.61	0.60	0.56	0.51	0.45	0.31
T/K	8	9	10	11	12	13	14	15
$\chi_T/\text{cm}^3 \text{ mol}^{-1}$	4.27	3.68	3.27	2.96	2.70	2.50	2.30	2.15
$\chi_S/\text{cm}^3 \text{ mol}^{-1}$	0.34	0.33	0.35	0.30	0.28	0.25	0.25	0.23
$\tau/\mu\text{sec}$	15740	8830	5650	3580	2410	1610	1160	808
α	0.26	0.23	0.18	0.16	0.15	0.14	0.11	0.11
T/K	16	17	18	19	20	21	22	23
$\chi_T/\text{cm}^3 \text{ mol}^{-1}$	2.02	1.90	1.79	1.70	1.61	1.54	1.47	1.40
$\chi_S/\text{cm}^3 \text{ mol}^{-1}$	0.20	0.23	0.21	0.23	0.17	0.25	0.35	0.45
$\tau/\mu\text{sec}$	577	428	302	227	154	116	89.6	37.3
α	0.10	0.08	0.09	0.08	0.07	0.05	0.05	0.12
T/K	24	25	26					
$\chi_T/\text{cm}^3 \text{ mol}^{-1}$	1.34	1.29	1.23					
$\chi_S/\text{cm}^3 \text{ mol}^{-1}$	0.55	0.16	0.15					
$\tau/\mu\text{sec}$	35.2	21.6	12.9					
α	0.10	0.08	0.07					

Table S4. Wave functions with definite projection of the total moment $|m_J\rangle$ for the lowest two Kramers doublets (KDs) of individual Dy^{III} fragments for **1** and **2**.

	E/cm^{-1}	wave functions		
1	0.0	98% $ \pm 15/2\rangle$		
	202.0	90% $ \pm 13/2\rangle + 4\% \pm 11/2\rangle$		
2	0.0	97% $ \pm 15/2\rangle$		
	147.1	86% $ \pm 13/2\rangle + 5\% \pm 11/2\rangle + 4\% \pm 7/2\rangle$		

Table S5. Exchange energies (cm^{-1}) and main values of the g_z for the lowest two exchange doublets of complexes **1** and **2**.

	1		2	
	E/cm^{-1}	g_z	E/cm^{-1}	g_z

1	0.0	39.436	0.0	39.355
2	0.2	0.000	0.2	0.000

References

- (1) Casanova, D.; Llunell, M.; Alemany, P.; Alvarez, S. The rich stereochemistry of eight vertex polyhedra: a continuous shape measures study. *Chem. Eur. J.* **2005**, *11*, 1479-1494.
- (2) Aubin, S. M. J.; Sun, Z.; Pardi, L.; Krzystek, J.; Folting, K.; Brunel, L.-C.; Rheingold, A. L.; Christou, G.; Hendrickson, D. N. Reduced anionic Mn₁₂ molecules with half-integer ground states as single molecule magnets. *Inorg. Chem.* **1999**, *38*, 5329-5340.